Article

pubs.acs.org/Biomac

Controlling Surface Topology and Functionality of Electrospun Fibers on the Nanoscale using Amphiphilic Block Copolymers To Direct Mesenchymal Progenitor Cell Adhesion

Priyalakshmi Viswanathan,[†,‡,○] Efrosyni Themistou,[‡,§,∥,○] Kamolchanok Ngamkham,[⊥] Gwendolen C. Reilly,[#] Steven P. Armes,[§] and Giuseppe Battaglia*[,⊥]

[†]The Krebs Institute, [‡]Department of Biomedical Sciences, University of Sheffield, Sheffield, South Yorkshire S10 2TN, United Kingdom

[§]Department of Chemistry, University of Sheffield, Sheffield, South Yorkshire S3 7HF, United Kingdom

[∥]School of Chemistry and Chemical Engineering, Queen's University Belfast, Belfast BT9 5AG, United Kingdom

[⊥]Department of Chemistry, University College London, London WC1H 0AJ, United Kingdom

[#]INSIGNEO Institute for in Silico Medicine, Department of Materials Science and Engineering, University of Sheffield, Sheffield, South Yorkshire S3 7HQ, United Kingdom

Supporting Information

ABSTRACT: Surface patterning in three dimensions is of great importance in biomaterials design for controlling cell behavior. A facile one-step functionalization of biodegradable PDLLA fibers using amphiphilic diblock copolymers is demonstrated here to systematically vary the fiber surface composition. The copolymers comprise a hydrophilic poly[oligo(ethylene glycol) methacrylate] (POEGMA), poly[(2-methacryloyloxy)ethyl phosphorylcholine] (PMPC), or poly[2-(dimethylamino)ethyl methacrylate)] (PDMAEMA) block and a hydrophobic poly(L-lactide) (PLA) block. The block copolymer-modified fibers have increased surface hydrophilicity compared to that of PDLLA fibers. Mixtures of PLA–PMPC and PLA–POEGMA copolymers are utilized to exploit microphase separation of the incompatible hydrophilic PMPC and POEGMA blocks at the fiber surface. Conjugation of an RGD cell-adhesive peptide to one hydrophilic block (POEGMA) using thiol-ene chemistry produces fibers with domains of cell-adhesive (POEGMA) and cell-inert (PMPC) sites, mimicking the adhesive properties of the extracellular matrix (ECM). Human mesenchymal progenitor cells (hES-MPs) showed much better adhesion to the fibers with surface-adhesive heterogeneity compared to that to fibers with only adhesive or only inert surface chemistries.

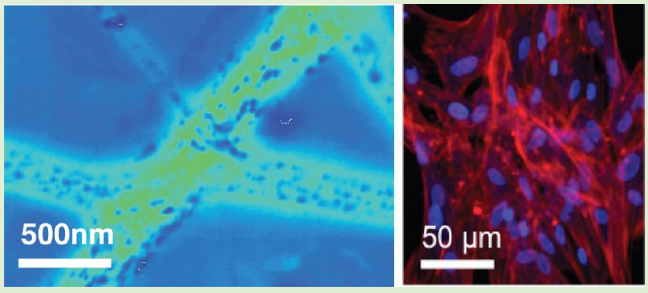

INTRODUCTION

The cell–material interface has been shown to have considerable influence on cell behavior such as adhesion, proliferation, and differentiation. In biological tissues, many of these physicochemical cues are provided by the extracellular matrix (ECM). The ECM is a complex network that presents multiple repeated adhesive motifs heterogeneously spaced and organized on the nanometer scale, which changes dynamically from protein folding and unfolding.[1] Often, this level of spatial organization is limited in synthetic substrates where presentation of ligands is homogeneously spaced with specific geometries and is presented in 2D.[2−5] Previous studies have shown, by fluorescence labeling, that cell binding sites in fibroblast-derived fibronectin are heterogeneously spaced,[6,7] although initial cell attachment can further expose synergistic binding sites.[8,9] Additionally, nanotopographies arranged in a semirandom geometry can direct osteogenic differentiation[10] of human mesenchymal stem cells (hMSCs), but not on square planar or hexagonal geometries. Therefore, the synthesis and design of 3D matrices that mimic both the structural aspects and adhesive heterogeneity of the ECM is of great interest in controlling cell behavior at the molecular level.

Electrospinning is a versatile and facile process for generating fibrous mats from various synthetic and natural polymers, which have been used as porous matrices for tissue engineering applications.[11,12] The morphology and alignment of such fibers have been extensively studied.[12,13] However, the biodegradable polymers commonly used in tissue engineering such as PLA, polycaprolactone (PCL), and poly(lactic-*co*-glycolide) (PLGA) are relatively hydrophobic, and enhancing their wettability through surface functionalization is desirable. Potential strategies for surface functionalization include plasma treat-

Received: May 9, 2014
Revised: November 17, 2014
Published: November 17, 2014

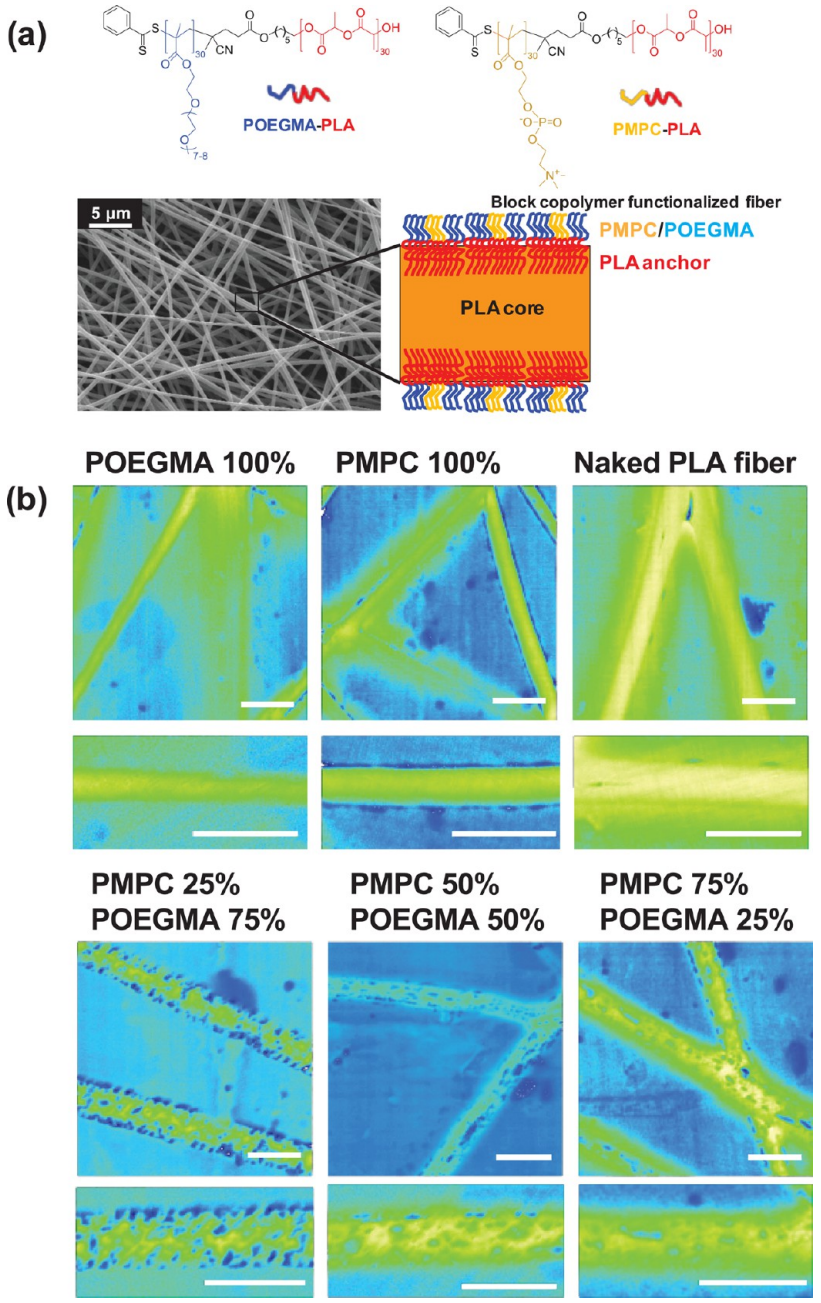

Figure 1. Surface engineering of electrospun fibers. (a) Surface functionalization of P*DL*LA electrospun fibers by incorporation of POEGMA−PLA and PMPC−PLA amphiphilic linear diblock copolymers. (b) POEGMA−PLA and PMPC−PLA diblock copolymers mixed in various molar ratios can induce microphase separation at the solid−water interface to generate 3D fibers with topologically defined surfaces expressed in terms of PMPC and POEGMA mol %. Fibers were imaged by SEM using backscattered electron imaging (BEI). Scale bar = 500 nm.

ment,[14] polymer grafting,[15] physisorption,[16] and chemisorption.[17] Despite these efforts, the efficiency of surface functionalization could be significantly improved, as multiple processing steps using these strategies can reduce the reproducibility of surface functionalization and limit their usefulness for scaling-up materials fabrication for tissue engineering processes.

In principle, efficient surface functionalization of fibers can be achieved via a one-step protocol by electrospinning relatively high concentrations of amphiphilic diblock copolymers, such as poly(ethylene oxide)-*b*-polycaprolactone (PEO−PCL), since this results in segregation of the PEO chains at the fiber surface.[18] Alternatively, electrospinning high molecular weight (MW) homopolymers (e.g., PCL, PLA, PLGA) blended with hydrophobic, hydrophilic, or amphiphilic additives (e.g., block copolymers) at low concentrations can result in fibers with useful surface properties, such as superhydrophobicity,[19,20] hydrophilicity,[21−24] or light-responsive switchable wettability.[25] The Becker group has recently prepared electrospun nanofibers based on polymers synthesized using an amine-derivatized cyclooctine (4-dibenzocyclooctynol) as initiator for ring-opening polymerization.[26] This kind of end-functional PLA nanofiber can be derivatized postfabrication with peptides such as Tyr-Ile-Gly-Ser-Arg (YIGSR) using metal-free alkyne−azide cycloaddition.[27] Surface segregation of the additive is believed to occur because of its polarizable groups.[28,29] Charged

dx.doi.org/10.1021/bm500671j | *Biomacromolecules* 2015, 16, 66−75

additives can also increase solution conductivity and improve the likelihood of surface segregation.[20] In all of these examples, electrospun fibers present homogeneous surfaces that usually lack biospecific motifs that are known to be important for cell and tissue culture. Conjugation of cell-adhesive peptides, such as RGD[22,30] or carbohydrates,[31] can promote cell adhesion. However, such methods often lack spatial control of cell binding sites and hence can differ from that of native ECM,[6,8] making the subsequent cell response to the biomaterial suboptimal.

Spatial patterning of surface chemistry, for example, proteins in two-dimensional substrates, has been shown to influence human mesenchymal stem cell (hMSC) adhesion and differentiation.[32,33] Moreover, we have recently demonstrated the fabrication of three-dimensional foams expressing spatially controlled cell-adhesive motifs by exploiting the self-assembly of amphiphilic diblock copolymers at an oil−water interface to fine-tune hMSC adhesion.[6]

In the present study, we design highly porous 3D matrices with specific surface chemistry and topology. This strategy involves amphiphilic diblock copolymer self-assembly at the solid−air interface of poly(D,L-lactide) (P*DL*LA) electrospun fibers (Figure 1a). Herein, we demonstrate the facile surface functionalization of P*DL*LA fibers using the biocompatible amphiphilic diblock copolymers poly[(2-methacryloyloxy)ethyl phosphorylcholine]-*b*-poly(L-lactide) (PMPC−PLA), poly-[oligo(ethylene glycol) methacrylate]-*b*-(poly(L-lactide) (POEGMA−PLA), and poly[2-(dimethylamino)ethyl methacrylate)]-*b*-poly(L-lactide) (PDMAEMA−PLA), where L-lactide is the (3*S*)-cis-3,6-dimethyl-1,4-dioxane-2,5-dione (*LL*A) monomer.

First, the diblock copolymer composition required to induce surface segregation of the hydrophilic block is determined by varying the degree of polymerization of the PLA block for a model amphiphilic PDMAEMA−PLA diblock copolymer. The effect of fiber surface modification on surface wettability, resistance to protein adsorption, and long-term hydrolytic degradation is investigated and compared to that of hydrophobic P*DL*LA fibers. Second, we propose that mixing two different amphiphilic diblock copolymers, POEGMA−PLA and PMPC−PLA, in various molar ratios induces microphase separation of the hydrophilic POEGMA and PMPC blocks at the fiber surface (Figure 1b). This allows a range of functionalized 3D surfaces to be engineered. Both PMPC and POEGMA are known to strongly resist cell adhesion and protein adsorption.[34,35] Here, the cell-adhesive peptide, RGD, is conjugated to one of the hydrophilic blocks (the POEGMA block) using thiol-ene chemistry.[36−38] This allows the investigation of the effects of surface adhesive heterogeneity on human embryonic derived-mesenchymal progenitor (hES-MP) cell adhesion and morphology.

EXPERIMENTAL SECTION

Materials. Chloroform ($CHCl_3$), methanol (MeOH), trypsin−EDTA, Triton X-100, and tris(2-carboxyethyl)phosphine hydrochloride (TCEP, purum, ≥98.0%) were purchased from Sigma-Aldrich (UK). High MW (300 kDa) poly(D,L-lactide) (P*DL*LA) was obtained from Polysciences Inc. (USA). *N*,*N*-Dimethylformamide (DMF, chromatography grade) was purchased from Fisher Scientific (Loughborough, UK). The NH_2-RGDC-acid (RGDC peptide) and the NH_2-RDGC-acid (scrambled RDGC peptide with terminal cysteine) tripeptides were purchased from Pepceuticals (UK). Human embryonic stem cell-derived mesenchymal progenitors (hES-MP) were purchased from Cellectics, UK. Alpha-modified minimum essential medium (Alpha-MEM) was obtained from Gibco (UK), and fetal bovine serum (FBS), from BioSera. Penicillin/streptomycin and basic fibroblast growth factor (b-FGF) were both purchased from Invitrogen (UK). Bovine serum albumin (BSA)-conjugated Alexa Fluor 594, Phalloidin Texas Red, and DAPI were obtained from Molecular Probes (UK). All of the above reagents were used as received.

The preparation and characterization of the linear amphiphilic diblock copolymers PDMAEMA−PLA, POEGMA−PLA, and PMPC−PLA and of the vinyl sulfone-functionalized VSTEMA−POEGMA−PLA copolymer are described in our previous work.[38] These biodegradable copolymers were synthesized by a combination of two living polymerization techniques, namely, metal-free ring-opening polymerization (ROP) polymerizing (L-lactide)[39,40] and reversible addition−fragmentation chain transfer (RAFT) polymerization[41−43] for the methacrylic block. A two-step sequential polymerization procedure (Schemes S1-2, Supporting Information) was utilized for the PMPC−PLA synthesis.[38] A one-step simultaneous polymerization was used for the synthesis of PDMAEMA−PLA and POEGMA−PLA linear amphiphilic diblock copolymers (Scheme S1-1, Supporting Information) and also the POEGMA−PLA branched amphiphilic diblock copolymer (Scheme S2, Supporting Information), the precursor of the VSTEMA−POEGMA−PLA copolymer. This branched diblock copolymer consisted of disulfide branch points[44] formed by a cleavable disulfide-based dimethacrylate (DSDMA)[45−47] branching monomer. Cleavage of the disulfide bonds using excess tributylphosphine afforded 2-thioethyl methacrylate (TEMA) units (two TEMA units per DSDMA unit) and resulted in the formation of a thiol-functionalized PLA_{30}−P($OEGMA_{30}$-*stat*-$TEMA_2$) linear diblock copolymer (Scheme S3a, Supporting Information). The latter was reacted with a large excess of divinyl sulfone (DVS), allowing the conversion of the TEMA units to VSTEMA units and the formation of the vinyl sulfone-functionalized VSTEMA−POEGMA−PLA linear diblock copolymer (Scheme S3b, Supporting Information).

Methods. *Preparation and Morphological Characterization of Electrospun Diblock Copolymer-Functionalized PDLLA Fibers.* Solutions for electrospinning were prepared as follows: 1.9 μmoles of amphiphilic diblock copolymer (PMPC−PLA, POEGMA−PLA, or PDMAEMA−PLA) was mixed with 100 mg (0.3 μmoles) of P*DL*LA homopolymer (300 kDa) and 1.0 mL of solvent mixture. $CHCl_3$/MeOH (2:1 v/v) was used for preparing 10% w/v solutions of PMPC−PLA and POEGMA−PLA, and $CHCl_3$/DMF (3:1), for PDMAEMA−PLA solutions. Solutions of 100 mg of P*DL*LA homopolymer controls in 1.0 mL solutions (10% w/v) of both $CHCl_3$/DMF (3:1 v/v) and $CHCl_3$/MeOH (2:1 v/v) were also prepared. The resulting viscous solutions were electrospun as a blend using a custom-made horizontal rig with a rotating collector covered with an aluminum foil. The needle tip-to-collector distance was maintained at 15 cm, and the applied voltage was 20 kV. The solution was ejected at a rate of 1 mL/h, and, in all cases, random nonwoven mats were collected. Similarly, electrospun P*DL*LA fibers surface-functionalized with mixtures of PLA−POEGMA and PLA−PMPC diblock copolymers were prepared. More specifically, 1.9 μmoles of various amphiphilic diblock copolymer mixtures (with POEGMA/PMPC molar ratios of 75:25, 50:50, and 25:75) were dissolved in turn in 1.0 mL of a $CHCl_3$/MeOH (2:1 v/v) solvent mixture. The resulting copolymer solution was electrospun using the same electrospinning parameters as above.

Fibers were prepared for scanning electron microscopy (SEM) imaging by placing small sections on an aluminum stub with an adhesive carbon pad. Samples were coated with a gold overlayer (approximately 15 nm) using an Edwards S150B sputter coater. Fiber imaging was performed using a Philips XL20 scanning electron microscope at an accelerating voltage of 10 kV and a spot size of 3.0 nm. Average fiber diameters were measured for at least 100 fibers from a minimum of three micrographs using ImageJ software.

Linear RGDC and Scrambled RDGC Peptide Conjugation on Electrospun Vinyl Sulfone VSTEMA−POEGMA−PLA Diblock Copolymer-Functionalized PDLLA Fibers. The unreacted second double bond of the divinyl sulfone in the vinyl sulfone-functionalized linear

diblock copolymer VSTEMA−POEGMA−PLA (Scheme S3b, Supporting Information) can be used for conjugation with thiol-containing molecules,[48] such as cysteine-containing peptides. Here, linear RGDC and scrambled RDGC peptides with a terminal cysteine residue were conjugated to VSTEMA−POEGMA−PLA after electrospinning using the following protocol: Fibrous 2 × 2 cm^2 mats were cut and placed in 6-well plates covered with parafilm. Each 6-well plate was purged with nitrogen gas for 5 min. A solution of 0.36 mg of RGDC (or scrambled DRGC) peptide in 8 mL of PBS (45 μg/mL) and an 8 mL solution of TCEP in PBS (2.5 μg/mL) were placed in a 30 mL glass vial equipped with a magnetic stir bar and sealed with a rubber septum. The resulting solution (RGD/TCEP molar ratio = 10.5) was purged with nitrogen for 30 min, and a 2.0 mL aliquot was added under a nitrogen atmosphere to each well. The solution covering each fibrous mat was purged with nitrogen for a further 10 min and left covered at room temperature on a plate rocker for 4 h to allow conjugation to occur. After that, the fibers were washed three times with cold PBS solution. Fibers were then sterilized with cold 70% ethanol (EtOH) and air-dried prior to cell seeding. This protocol was repeated for all amphiphilic diblock copolymer mixtures of PMPC−PLA and VSTEMA−POEGMA−PLA.

Effect of PLA Block Length on Surface Functionalization with Amphiphilic Diblock Copolymers. To study the effect of the hydrophobic block length on the efficiency of surface functionalization, PDMAEMA−PLA was chosen as a model amphiphilic diblock polymer. PDMAEMA−PLA amphiphilic diblock copolymers[38] with various block lengths and MWs were used (Table S1, Supporting Information). Electrospinning processing conditions were maintained as before with a needle tip-to-collector distance of 15 cm at 20 kV. The resulting fiber diameters were determined using SEM. Water contact angles were measured using Milli-Q water at pH 7 and 10 (adjusted with 0.10 M NaOH) to examine how surface wettability varied with solution pH.

Fiber Degradation. Degradation rates for all diblock copolymer-functionalized fibers were investigated and compared to those of nonfunctionalized P*DL*LA fibers processed under the same solvent conditions. For example, fibers consisting of POEGMA−PLA and PMPC−PLA were compared to P*DL*LA fibers electrospun from a 2:1 $CHCl_3$/MeOH solution. For fibers consisting of $PDMAEMA_{25}$−PLA_{26}, $PDMAEMA_{30}$−PLA_{41}, or $PDMAEMA_{28}$−PLA_{48}, P*DL*LA fibers electrospun from a 3:1 $CHCl_3$/DMF solution were used as the control.

All fibers were first sterilized in cold 70% EtOH and rinsed in cold PBS buffer prior to the degradation studies. Three 10−20 mg samples of randomly aligned fiber meshes for each formulation were weighed prior to degradation. Samples were placed in a centrifuge tube under physiological conditions (PBS solution, 37 °C water bath). The PBS was replenished twice per week to maintain physiological pH, as P*LL*A/P*DL*LA is known to degrade faster under acidic or basic conditions.[49] At specific time points (days 1, 7, 14, 21, and 28), fibers were washed three times in deionized water and vortexed to ensure removal of all soluble degradation products. Fibers were then dried in a vacuum oven at room temperature for 72 h and reweighed to determine their mass loss. A total of three measurements for each time point were taken to determine an average mass loss. An extra sample that was washed in deionized water but not vortexed was imaged by SEM to assess the morphology of the degraded fibers. Degradation studies were repeated three times (n = 9).

Qualitative Assessment of Protein Adsorption. Fiber mats were sterilized using cold 70% EtOH and rinsed immediately three times with 1 mL of PBS. Mats of 1.5 × 1.5 cm^2 dimensions were incubated with 200 μL of AlexaFluor 594 BSA solution in PBS (100 μg/mL) for either 30 min or 2 h. Fibers were then washed thoroughly three times in PBS. Protein adsorption was qualitatively assessed by a Zeiss LSM510 Meta inverted confocal laser scanning microscope using a 25× objective lens, with untreated fibers being used as a control in each case.

Wettability of Electrospun Fibers. Static contact angles were measured using a Rame-Hart goniometer. 4−5 μL of Milli-Q water at pH 7 or 10 (adjusted using 0.1 M NaOH) was added on 1 × 1 cm^2 mats of electrospun fibers placed on a glass coverslip. A total of 3−4 measurements was taken for each fiber composition. Note that for such surfaces that exhibit porosity water contact angles serve as an indication of a change in surface wettability rather than as a measurement of surface tension. Surface roughness can increase the contact angle for hydrophobic surfaces above 90° and reduce the contact angle for hydrophilic surfaces below 90°.[50]

Detection of Phase-Separated Surface Domains. In order to visualize phase separation on fiber surfaces, we selectively stained one of our copolymers, VSTEMA−POEGMA−PLA, with phosphotungstic acid (PTA). A filtered 0.75% PTA solution in water (pH 7) was stained on electrospun fibers with different amphiphilic diblock copolymer mixtures for 3 s. After the excess solution was removed by blotting the grid using filter paper, samples were dried in vacuum oven overnight. SEM imaging was then performed using backscattered electron imaging (BEI) mode in JEOL 6700F field-emission scanning electron microscope. Uncoated samples were placed on an aluminum stub with adhesive carbon pad and imaged at an accelerating voltage of 5 kV and beam current of 10 μA. Heavier elements (PTA stained area) will appear brighter than the lighter ones. All images were processed, and the size of patches in each formulation was quantified from two independent sets of electrospun fibers using ImageJ.

3D Cell Culture and Adhesion of hES-MPs. Human embryonic stem cell-derived mesenchymal (or mesodermal) progenitors (hES-MP) were used for all studies. We chose hES-MPs as the model cell line for our experiments because they provide a homogeneous population of multipotent cells and have been shown to behave in a similar way to that of adult human mesenchymal stem cells (hMSCs) *in vitro* but without donor variability. They have been shown to differentiate toward osteogenic, chondrogenic, and adipogenic lineages[51,52] and to produce the bone cell markers alkaline phosphatase and mineralized matrix, as shown in a previous study in our laboratory.[53] According to the supplier, hES-MPs are positive for CD105, CD166, CD13, and CD10 and are negative for CD133 and CD117 surface antigens. The hES-MP cells were cultured in Alpha-MEM supplemented with 10% FBS and 1% penicillin/streptomycin. Basic fibroblast growth factor (b-FGF) (10 ng/mL) was also added to culture flasks during expansion but not during experiments. Cells were maintained in a humidified 37 °C incubator under 5% CO_2. Cultures were passaged at 70−80% confluence using trypsin−EDTA and split at a 1:5 ratio, and media were replenished every 2−3 days. Passages from 5 to 15 and basal media (without b-FGF) were used for all experiments in this study.

Fiber mats of 2 × 2 cm^2 dimensions were first sterilized in cold 70% EtOH and rinsed immediately three times with 1 mL of PBS solution. hES-MPs were trypsinized and seeded onto fibrous mats at a density of 2500 cells cm^{-2}. After 7 days of culture, cells were fixed in 3.7% formaldehyde for 20 min followed by permeabilization with 0.1% Triton X for 10 min. The actin cytoskeleton (f-actin) was stained with Phalloidin Texas Red (1:100), and the nucleus was stained with 25 μL of mounting medium containing DAPI. Cell morphology was visualized using an ImageExpress fluorescent microscope (Axon Instruments, UK) at 40× magnification.

RESULTS AND DISCUSSION

Fiber Morphology and Wettability. To investigate the optimum copolymer composition required to obtain surface segregation, a series of six PDMAEMA−PLA diblock copolymers of varying hydrophobic block lengths and MWs (Table S1, entries 1−6, Supporting Information) were electrospun as a blend with P*DL*LA homopolymer from a 3:1 v/v $CHCl_3$/DMF mixture. PDMAEMA copolymers have the dual advantage of being relatively easy to synthesize and pH responsive. The latter allows their surface properties to be controlled by changing the solution pH. The copolymer with the lowest hydrophobic content, $PDMAEMA_{25}$−PLA_{26}, not only produced the finest fibers (mean diameter = 312 ± 52 nm; Figure 2a,b) but also the highest wettability at pH 7 (Figure

dx.doi.org/10.1021/bm500671j | Biomacromolecules 2015, 16, 66−75

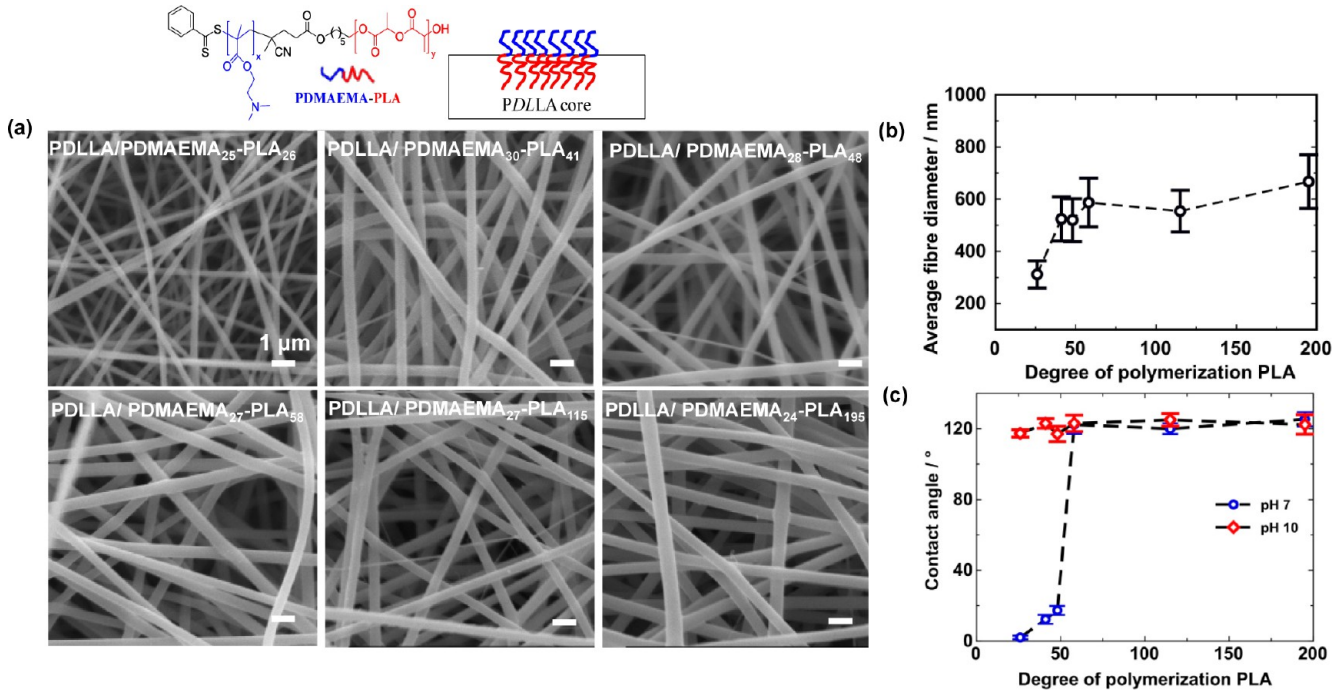

Figure 2. Scaffold morphology and wettability. (a) Representative scanning electron micrographs of PDMAEMA−PLA-functionalized fiber morphologies with varying PLA block lengths. (b) Average fiber diameter and (c) static contact angles obtained at pH 7 and 10 for PDMAEMA−PLA-functionalized fibers as a function of PLA degree of polymerization. Scale bar = 1 μm.

2c). Both $PDMAEMA_{30}$−PLA_{41} and $PDMAEMA_{28}$−PLA_{48} also produced fibers with surface hydrophilic characteristics, with static contact angles of 12 ± 2° and 17 ± 2° at pH 7, respectively (Figure 2c), although larger mean fiber diameters of 523 ± 92 and 512 ± 91 nm, respectively, were obtained (Figure 2b). However, all other PDMAEMA−PLA formulations only led to poorly wettable, relatively hydrophobic composite fibers. The pH-dependent wettability behavior of fibers functionalized with PDMAEMA (average $pK_a \sim 7.5$[54]) was further demonstrated by the relatively large contact angles obtained at pH 10, which is indicative of a hydrophobic surface. A linear relationship between the hydrophobicity of the electrospun fibers and their PLA content was not observed. Instead, there was an abrupt increase in contact angle at pH 7 from PLA_{48} to PLA_{58} corresponding to PLA molar fractions between 0.61 to 0.66. Similar sharp transitions were observed in other polymer surface segregation.[55] The surface segregation of the diblock copolymers is driven by incompatibility between the matrixphobic block (in this case the PDMAEMA) and the PLA matrix. Inevitably, the longer the PLA (i.e., the higher the PLA molar fraction), the more the diblock copolymer is soluble within the PLA matrix. It is worth noticing that, even though the fiber formation occurs on the millisecond time scale,[12] the diblock copolymer has enough mobility to segregate at the fiber surface and change its wettability.

Similar diblock compositions, e.g., $PMPC_{25}$−PLA_{25} and $POEGMA_{29}$−PLA_{29}, corresponding to PLA molar fractions of 0.33 and 0.29, were thus utilized in all further experiments to promote surface functionalization. Figure 3 shows the morphologies and contact angle data at pH 7 for electrospun fibers obtained from $PMPC_{25}$−PLA_{25} or $POEGMA_{29}$−PLA_{29} and P*DL*LA blends. For both copolymers, the resulting fibers were found to be highly hydrophilic, with minimal contact angles at pH 7 (Figure 3b) compared to that of the intrinsically hydrophobic P*DL*LA fibers (contact angle = 120° ± 4°). However, these fibers proved to be significantly thicker, with mean fiber diameters of 872 ± 210 and 931 ± 127 nm, respectively, compared to that of $PDMAEMA_{25}$−PLA_{26} fibers (312 ± 52 nm).

In all cases, the amphiphilic diblock copolymer additive resulted in fibers that were readily wettable in water, thus confirming their hydrophilic surface character. It has been previously shown that the choice of solvent promotes surface migration of hydrophilic species.[56,57] Polar solvents such as MeOH and DMF serve two purposes. First, they can increase jet stability during electrospinning to produce more homogeneous fibers and prevent electrospraying.[58] Second, enhanced solubility of the amphiphilic additive can drive surface segregation of the hydrophilic component after solvent evaporation.[18] Additionally, surface-active molecules such as amphiphilic block copolymers have been shown to segregate at the fiber−air interface to minimize the surface free energy.[19]

Fiber Degradation. The hydrolytic degradation of aliphatic polyesters such as P*LL*A and P*DL*LA have been extensively studied, as these biodegradable polymers are widely used for various biomedical applications.[11,59] Polylactides undergo a bulk degradation mechanism via random scission of the ester backbone with the lactic acid byproduct being metabolized during the Krebs cycle.[60] However, a high local concentration of acidic degradation byproducts, often noted for bulk-eroding polymers during the latter stages of degradation, has been shown to produce cytotoxicity.[22,60] There are many techniques that render the surface of electrospun fibers more hydrophilic in order to control cell attachment, media flow, or bioactivity.[8,9] However, there are few reports focusing on the influence of hydrophilic additives on the hydrolytic degradation of hydrophobic copolymers.[18] Thus, in this work, the degradation profile of diblock copolymer-functionalized fibers was studied for 1 month under physiological conditions.

dx.doi.org/10.1021/bm500671j | *Biomacromolecules* 2015, 16, 66−75

(a)

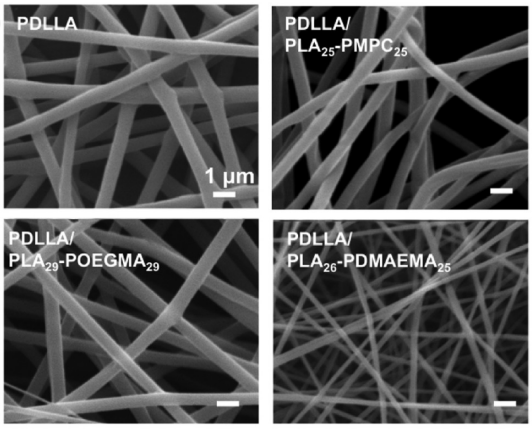

(b)

	Fiber diameter / nm	Contact angle / °
PDLLA	893 ± 143	120 ± 4
PDLLA/ PLA_{25}-$PMPC_{25}$	872 ± 210	1 ± 1
PDLLA/ PLA_{26}-$PDMAEMA_{25}$	312 ± 52	2 ± 1
PDLLA/ PLA_{29}-$POEGMA_{29}$	931 ± 127	2 ± 1

Figure 3. Morphology and wettability of electrospun fibers. (a) Representative scanning electron micrographs and (b) mean fiber diameters and static contact angles at pH 7 of diblock copolymer-functionalized electrospun fibers compared to that of P*DL*LA fibers. Scale bar = 1 μm.

P*DL*LA fibers appeared to swell upon wetting with PBS at 37 °C from the first day (Figure 4a) such that, after 28 days, P*DL*LA fibers appear fused together, with complete loss of porosity. Hydrolytic degradation, however, indicated little or no mass loss of 0.17 ± 0.015% on day 1 and 1.83 ± 0.83% by day 28. On the other hand, copolymer-functionalized fibers maintained much of their original morphology while becoming swollen during the same time period. Hydrolytic degradation indicated mass loss after day 1 of 9.0 ± 1.2% for POEGMA–PLA and 7.0 ± 1.2% for PMPC–PLA (Figure 4b). Mass loss by day 28 was 20.2 ± 2.1 and 17.2 ± 1.8% for POEGMA–PLA and PMPC–PLA, respectively.

Similarly, those PDMAEMA–PLA-functionalized fibers exhibiting high wettability (Figure 2c) were subjected to hydrolytic degradation. Mass loss was observed after day 1, which continued over a 4 week period (Figure S1b, Supporting Information), regardless of the PLA block length. Fiber morphologies (Figure S1a, Supporting Information) did not appear to change significantly over 28 days compared to that of P*DL*LA control fibers, which showed loss of porosity and swollen fibers over the same time period. Again, P*DL*LA fibers exhibited no significant mass loss over the first 28 days, although they displayed the greatest change in morphology compared to that of copolymer-functionalized fibers (Figure S1a,b, Supporting Information). This is due to the fact that P*DL*LA is hydrophobic and is known to undergo a bulk degradation mechanism.[60]

In contrast, it is expected that the hydrophilic copolymer-functionalized fibers alter the rate of fiber degradation.[49] The rapid mass loss in the first 28 days suggests cleavage of PLA from the diblock copolymer, resulting in loss of the entire hydrophilic block (Scheme S4, Supporting Information). This, in theory, leads to complete loss of surface functionalization within the first month for POEGMA–PLA (see Supporting Information for calculated mass loss), since surface segregation is a result of physical entanglement of the copolymer chains within the P*DL*LA matrix. Grafahrend et al. showed that surface functionalization of PLGA fibers using a six-arm star-shaped PEG macromolecule increased the rate of fiber degradation at longer times compared to that of PLGA alone.[22] In contrast to our study, covalently attached hydrophilic additives did not show significant initial mass loss,[15,22] although they did increase the overall rate of degradation. In our study, fiber mass loss continued to increase after this period, despite the likely loss of the hydrophilic block. This is probably because of the higher

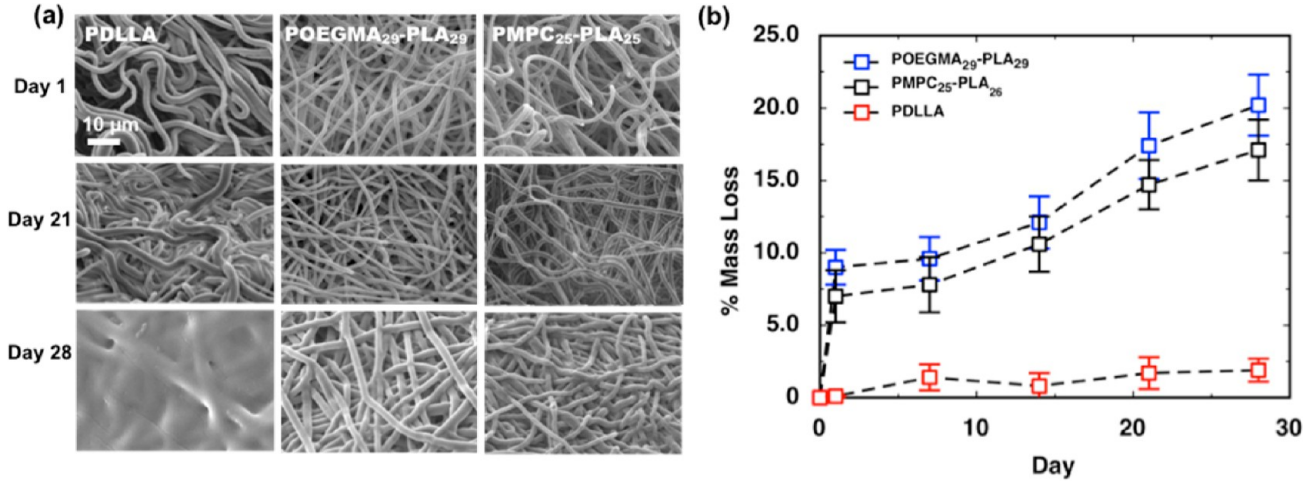

Figure 4. Fiber degradation. Degradation curves obtained for surface-functionalized fibers. (a) Scanning electron micrographs of diblock copolymer-functionalized fibers after degradation under physiological conditions for 1, 21, and 28 days. (b) Percentage mass loss observed for copolymer-modified fibers over 28 days compared to that of P*DL*LA control fibers. n = 9, ±SD. Scale bar = 10 μm.

dx.doi.org/10.1021/bm500671j | *Biomacromolecules* 2015, 16, 66–75

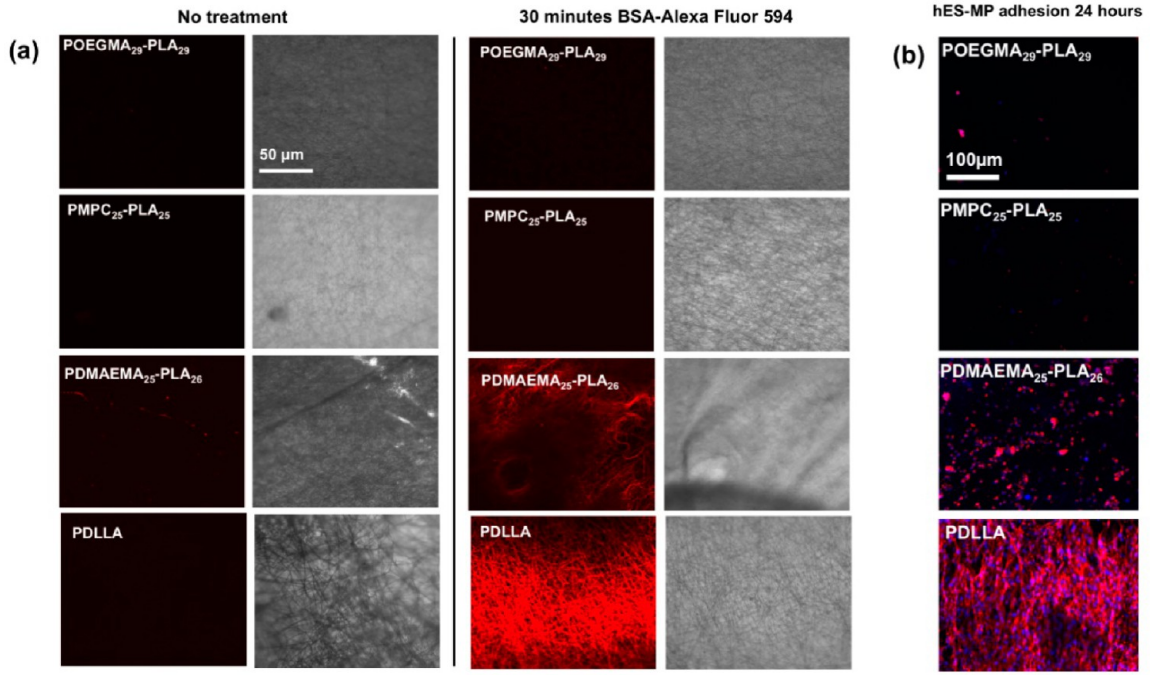

Figure 5. Nonspecific protein adsorption and cell adhesion. (a) Adsorption of BSA-conjugated Alexa Fluor 594 on diblock copolymer-functionalized fibers after 30 min; scale bar = 50 μm. (b) Human mesenchymal progenitors (hES-MPs) cultured on diblock copolymer-functionalized fibers for 24 h. Cells were stained for the nucleus in blue (DAPI) and f-actin in red (Phalloidin Texas Red); scale bar = 100 μm. n = 6.

wettability of copolymer-modified fibers, which increases the access of water to the P*DL*LA matrix and therefore increases its rate of hydrolysis. It is expected that once surface functionality is lost the fiber lactide core degrades by a bulk erosion mechanism.

Differential Protein and Stem Cell Adhesion Based on Surface Chemistry. Amphiphilic diblock copolymer surface functionalization resulted in relatively hydrophilic fiber surfaces for all diblock copolymers examined in this study compared to the inherent hydrophobicity of the P*DL*LA matrix. Thus, the effects of surface hydrophilicity and surface chemistry on protein resistance and cell adhesion were investigated. For fibers functionalized with a single diblock copolymer, such as PDMAEMA−PLA, PMPC−PLA, or POEGMA−PLA, BSA conjugated with Alexa Fluor 594 was incubated for 30 min, and protein adsorption was qualitatively evaluated by fluorescence microscopy. For fibers modified with either PMPC−PLA or POEGMA−PLA, no BSA adsorption was detected (Figure 5a); this was expected, as both PMPC and POEGMA are known to exhibit nonfouling properties.[34,35] In contrast, BSA adsorption was detected on both P*DL*LA fibers and PDMAEMA−PLA functionalized fibers (Figure 5a). This is not surprising, as nonspecific protein adsorption is known to occur[61,62] on hydrophobic surfaces such as P*DL*LA and cationic surfaces such as PDMAEMA. Thus, we show that a relatively small amount of block copolymer electrospun as a blend with a hydrophobic homopolymer results in large-scale surface functionalization in 3D.

Cell adhesion was evaluated by culturing hES-MPs for 24 h on copolymer-functionalized fibers and P*DL*LA fibers. As shown in Figure 5b, no cells were observed on either the POEGMA−PLA- or PMPC−PLA-modified fibers. Cells cultured on PDMAEMA−PLA became discernibly rounded after 24 h. It has been previously shown that cationic polymers can often result in cellular stress and cytotoxity.[63] In contrast, P*DL*LA fibers presented the highest number of well-spread hES-MPs, which is often noted for hydrophobic matrices.

By mixing PMPC−PLA and POEGMA−PLA diblock copolymers, the dissimilar hydrophilic blocks should undergo phase separation at the solid−air interface, forming surface domains of PMPC and POEGMA. We have previously shown that microphase separation of the double-hydrophilic diblock copolymers of PMPC and PEG[64] occurs in aqueous solution. Additionally, we and others have demonstrated this phenomenon for amphiphilic diblock copolymers both in solution and at the oil−water interface, resulting in microphase separation of both the hydrophobic[65] and hydrophilic blocks.[6,66,67] Here, to detect the phase separation between POEGMA and PMPC blocks, we acquired backscattered SEM micrographs (Figure 1b) of fibers stained with 0.75% PTA (pH 7). PTA reacts with vinyl sulfone groups and results in bright spots on backscattered electron images. Phase separation was not observed on any of the P*DL*LA, POEGMA 100%, or PMPC 100% fibers, but it was clearly noticed on copolymer mixtures, POEGMA 75%, POEGMA 50%, and POEGMA 25%. The area of the fibers that was covered with bright spots varied according to the molar ratio of POEGMA. The average size of patches occurred from phase separation is quite similar in each mixture (160.51 ± 52.99, 135.59 ± 87.99, and 145.97 ± 99.54 nm for POEGMA 75%, POEGMA 50%, and POEGMA 25%, respectively).

As both PMPC and POEGMA are known to resist protein adsorption and cell adhesion, we functionalized the POEGMA block with vinyl sulfone groups (Scheme S3, Supporting Information) to aid conjugation of thiol-containing cell-adhesive peptides such as RGDC (Figure 6a) via thiol-ene chemistry. Electrospun fibers were produced using the PMPC−PLA (as described above) and the vinyl sulfone-functionalized VSTEMA−POEGMA−PLA amphiphilic linear diblock copolymers, where VSTEMA is 2-(2-(vinylsulfonyl)ethylthio)ethyl methacrylate, and their mixtures. Three molar compositions

dx.doi.org/10.1021/bm500671j | *Biomacromolecules* 2015, 16, 66−75

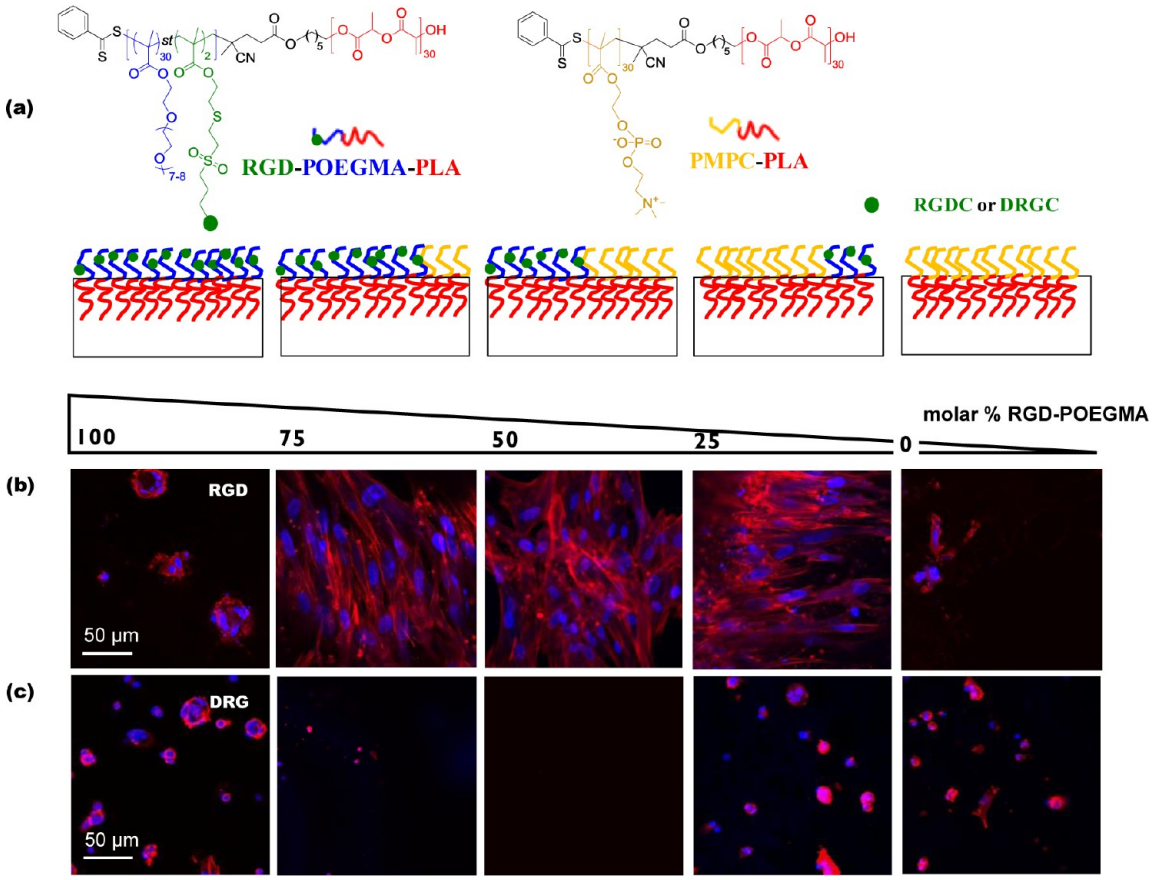

Figure 6. Differential cell adhesion. (a) Chemical structures of cell-adhesive RGD-vinyl sulfone-functionalized RGD−POEGMA−PLA and cell-inert PMPC−PLA amphiphilic linear diblock copolymers and spatial presentation of adhesive sites and inert sites on a P*DL*LA fiber surface as a function of the mol % of POEGMA. Human mesenchymal progenitors (hES-MPs) cultured for 7 days on diblock copolymer mixtures show differential spreading on (b) RGDC-functionalized fibers and limited spreading on (c) DRGC-functionalized fibers. Cells were stained for the nucleus in blue (DAPI) and f-actin in red (Phalloidin Texas Red). n = 6; scale bar = 50 μm.

(25:75, 50:50, and 75:25) of these two copolymers were generated, resulting in a series of P*DL*LA fibers with a range of surface chemistries and topologies. RGDC was conjugated after electrospinning by a thiol-ene reaction between its terminal cysteine thiol group and the pendent vinyl sulfone on the hydrophilic P(OEGMA$_{30}$-*stat*-VSTEMA$_2$) block (Scheme S3b, Supporting Information). Thus, in the present study, POEGMA100 corresponds to 100% cell-adhesive, whereas PMPC100 corresponds to 100% cell nonadhesive polymer. It is known that hydrophobic P*DL*LA/P*LL*A supports cell adhesion through the adsorption of serum proteins *in vitro*.[14,18] While it is relatively easy to produce polylactide-based 3D matrices, it is not easy to control cell interactions at the molecular level. The fibers produced here offer two distinct advantages for understanding cell-matrix interactions: (1) adhesive sites are heterogeneously spaced and can be readily controlled by the amount of POEGMA used in the copolymer mixture so as to better mimic the adhesive heterogeneity found in the ECM and (2) cell-specific adhesion occurs via RGD ligands conjugated to the POEGMA chains, whereas nonadhesive sites are rendered protein-resistant and cell-inert by the PMPC chains, allowing for direct assessment of cell−material interactions. To investigate the cellular response to copolymer-functionalized electrospun fibers, hES-MPs were cultured onto diblock copolymer-functionalized fibers. As cell shape is shown to be an early indicator of hMSC fate, we sought to examine if the adhesive heterogeneity would affect hES-MP cell morphology on these surfaces.

Cell morphologies and spreading were qualitatively evaluated (Figure 6b) after 7 days by staining the nucleus with DAPI and f-actin with Phalloidin Texas Red. Low cell numbers were observed on the cell-inert PMPC100 fibers, with limited cell spreading. hES-MPs formed clusters and adopted a rounded morphology on the cell-adhesive POEGMA100 fibers, despite this being the surface with the highest concentration of adhesive ligands. This is probably due to retardation of cell motility, which is known to occur on surfaces with RGD ligand concentrations above a certain threshold for adhesion.[68] hES-MPs were the most well-spread on all diblock copolymer mixtures (Figure 6b), where they appeared to be elongated in one direction and spindle-like in shape on both POEGMA25 and POEGMA75 fiber surfaces. For POEGMA50 fibers, cells displayed a higher degree of spreading in a nonaligned orientation in contrast to that with the other copolymer mixtures (Figure 6b). In fibers where the control scrambled DRGC sequence was conjugated, either a few rounded cells were detected or no cells at all were present for all compositions (Figure 6c).

Taken together, these results show that the mixing of two amphiphilic block copolymers allows the spatial arrangement of RGD ligands in a manner that more closely mimics the heterogeneous adhesive sites observed in native ECM molecules such as fibronectin.[6,69] Cell spreading was observed

dx.doi.org/10.1021/bm500671j | *Biomacromolecules* 2015, 16, 66−75

only on surfaces with copolymer mixtures, suggesting that a mixture of adhesive and nonadhesive chemical cues may be important to obtain optimal cell attachment and to modulate cell shape compared to surfaces with homogeneous chemistries. Cell adhesion to the ECM requires the ability to form focal adhesions through the recruitment and clustering of integrins. Synthetic 2D substrates have been previously designed with specific surface chemistries by controlling ligand affinity and density[70,71] at the molecular level. Such surfaces can influence cell responses such as shape and cytoskeletal tension and, as a result, direct stem cell fate. Similarly, the spatial arrangement of nanoscopic topologies, e.g., semirandom versus square planar, can either promote differentiation[10] or maintain multipotency[72] of hMSCs. Appropriate ligand spacing can either inhibit[73] or enhance[5] cell adhesion and spreading as a consequence of the dynamics of focal adhesion formation. In the present study, the 3D spatial presentation of ligands is defined and controlled by the phase-separated hydrophilic domains of the diblock copolymer additives. The resulting heterogeneous spacing, achieved by the mixing of two dissimilar block copolymers, contributes to the differential cell adhesion that is observed. Moreover, the distribution of adhesive sites in POEGMA25 and POEGMA75 affect cell spreading differently compared to that for cells cultured on POEGMA50. This suggests that the variation in adhesive spacing may affect cell adhesion dynamics in the context of hMSC lineage specification and warrants further study.

CONCLUSIONS

Electrospun P*DL*LA fiber modification to introduce hydrophilic surface character has been established via a facile one-step protocol using amphiphilic PLA-based diblock copolymers with the appropriate hydrophobic/hydrophilic balance. Enhanced degradation of the resulting surface-modified hydrophilic fibers compared to that of unmodified hydrophobic P*DL*LA fibers was observed. Low protein adsorption was obtained on fibers expressing POEGMA and PMPC chains. Furthermore, judicious mixing of two diblock copolymers (e.g., POEGMA−PLA and PMPC−PLA) generated a range of surface topologies by exploiting interface-confined copolymer phase separation. Introduction of cell-adhesive (RGD-POEGMA) and cell-inert (PMPC) hydrophilic domains on the fiber surface enabled direct assessment of cell−matrix interactions. The observed hES-MP cell adhesion and spreading dependence on surface chemistry and topology reflects the heterogeneity of adhesive binding sites found in the ECM. Thus, the ability to fine-tune the local adhesive properties of electrospun polymers provides a unique means of designing 3D scaffolds for potential applications in tissue engineering and regenerative medicine.

ASSOCIATED CONTENT

Supporting Information

Synthesis, characterization, and functionalization of amphiphilic diblock copolymers and degradation of diblock copolymer-functionalized fibers. This material is available free of charge via the Internet at http://pubs.acs.org.

AUTHOR INFORMATION

Corresponding Author

*E-mail: g.battaglia@ucl.ac.uk.

Author Contributions

○P.V. and E.T. contributed equally to this work.

Notes

The authors declare no competing financial interest.

ACKNOWLEDGMENTS

The authors would like to thank Dr. Robin Delaine-Smith for imaging assistance, and the Department of Biomedical Sciences at the University of Sheffield for use of the Electron Microscopy Unit. EPSRC (EP/I001697/1) and HFSP (RGY0064/2010) are gratefully acknowledged for providing financial support for this research.

REFERENCES

(1) Vogel, V.; Sheetz, M. *Nat. Rev. Mol. Cell Biol.* **2006**, *7*, 265−275.
(2) Frith, J. E.; Mills, R. J.; Cooper-White, J. J. *J. Cell Sci.* **2012**, *125*, 317−327.
(3) George, P. A.; Quinn, K.; Cooper-White, J. J. *Biomaterials* **2010**, *31*, 641−647.
(4) Chen, W.; Villa-Diaz, L. G.; Sun, Y.; Weng, S.; Kim, J. K.; Lam, R. H. W.; Han, L.; Fan, R.; Krebsbach, P. H.; Fu, J. *ACS Nano* **2012**, *6*, 4094−4103.
(5) Arnold, M.; Cavalcanti-Adam, E. A.; Glass, R.; Blümmel, J.; Eck, W.; Kantlehner, M.; Kessler, H.; Spatz, J. P. *ChemPhysChem* **2004**, *5*, 383−388.
(6) Viswanathan, P.; Chirasatitsin, S.; Ngamkham, K.; Engler, A. J.; Battaglia, G. *J. Am. Chem. Soc.* **2012**, *134*, 20103−20109.
(7) Engler, A. J.; Chan, M.; Boettiger, D.; Schwarzbauer, J. E. *J. Cell Sci.* **2009**, *122*, 1647−1653.
(8) Reilly, G. C.; Engler, A. J. *J. Biomech.* **2010**, *43*, 55−62.
(9) Vogel, V. *Annu. Rev. Biophys. Biomol. Struct.* **2006**, *35*, 459−488.
(10) Dalby, M. J.; Gadegaard, N.; Tare, R.; Andar, A.; Riehle, M. O.; Herzyk, P.; Wilkinson, C. D. W.; Oreffo, R. O. C. *Nat. Mater.* **2007**, *6*, 997−1003.
(11) Pham, Q. P.; Sharma, U.; Mikos, A. *Tissue Eng.* **2006**, *12*, 1197−1211.
(12) Greiner, A.; Wendorff, J. H. *Angew. Chem., Int. Ed.* **2007**, *46*, 5670−5703.
(13) Li, D.; Xia, Y. *Adv. Mater.* **2004**, *16*, 1151−1170.
(14) Yao, C.; Li, X.; Neoh, K. G.; Shi, Z.; Kang, E. T. *J. Membr. Sci.* **2008**, *320*, 259−267.
(15) Källrot, M.; Edlund, U.; Albertsson, A.-C. *Biomacromolecules* **2007**, *8*, 2492−2496.
(16) Casper, C. L.; Yamaguchi, N.; Kiick, K. L.; Rabolt, J. F. *Biomacromolecules* **2005**, *6*, 1998−2007.
(17) Park, K.; Ju, Y. M.; Son, J. S.; K, A.; Han, D. K. *J. Biomater. Sci., Polym. Ed.* **2007**, *18*, 369−382.
(18) Grafahrend, D.; Calvet, J. L.; Klinkhammer, K.; Salber, J.; Dalton, P. D.; Möller, M.; Klee, D. *Biotechnol. Bioeng.* **2008**, *101*, 609−621.
(19) Hardman, S. J.; Muhamad-Sarih, N.; Riggs, H. J.; Thompson, R. L.; Rigby, J.; Bergius, W. N. A.; Hutchings, L. R. *Macromolecules* **2011**, *44*, 6461−6470.
(20) Deitzel, J. M.; Kosik, W.; McKnight, S. H.; Beck Tan, N. C.; DeSimone, J. M.; Crette, S. *Polymer* **2002**, *43*, 1025−1029.
(21) Haamann, D.; Bispinghoff, M.; Hönders, D.; Suschek, C.; Möller, M.; Klee, D. *J. Appl. Polym. Sci.* **2012**, *125*, 3638−3647.
(22) Grafahrend, D.; Heffels, K.-H.; Beer, M. V.; Gasteier, P.; Möller, M.; Boehm, G.; Dalton, P. D.; Groll, J. *Nat. Mater.* **2010**, *10*, 67−73.
(23) Kim, K.-O.; Kim, B.-S.; Lee, K.-H.; Park, Y.-H.; Kim, I.-S. *J. Mater. Sci.: Mater. Med.* **2013**, *24*, 2029−2036.
(24) Cho, Y.; Cho, D.; Park, J. H.; Frey, M. W.; Ober, C. K.; Joo, Y. L. *Biomacromolecules* **2012**, *13*, 1606−1614.
(25) Chen, M.; Besenbacher, F. *ACS Nano* **2011**, *5*, 1549−1555.
(26) Zheng, J.; Liu, K.; Reneker, D. H.; Becker, M. L. *J. Am. Chem. Soc.* **2012**, *134*, 17274−17277.
(27) Smith Callahan, L. A.; Xie, S.; Barker, I. A.; Zheng, J.; Reneker, D. H.; Dove, A. P.; Becker, M. L. *Biomaterials* **2013**, *34*, 9089−9095.
(28) Sun, X. Y.; Shankar, R.; Börner, H. G.; Ghosh, T. K.; Spontak, R. J. *Adv. Mater.* **2007**, *19*, 87−91.

(29) Sun, X.-Y.; Nobles, L. R.; Börner, H. G.; Spontak, R. J. *Macromol. Rapid Commun.* **2008**, *29*, 1455−1460.
(30) Bockelmann, J.; Klinkhammer, K.; von Holst, A.; Seiler, N.; Faissner, A.; Brook, G. A.; Klee, D.; Mey, J. *Tissue Eng., Part A* **2011**, *17*, 475−486.
(31) Lancuški, A.; Bossard, F.; Fort, S. *Biomacromolecules* **2013**, *14*, 1877−1884.
(32) Khetan, S.; Burdick, J. A. *Biomaterials* **2010**, *31*, 8228−8234.
(33) DeForest, C. A.; Anseth, K. S. *Nat. Chem.* **2011**, *3*, 925−931.
(34) Yoshimoto, K.; Hirase, T.; Madsen, J.; Armes, S. P.; Nagasaki, Y. *Macromol. Rapid Commun.* **2009**, *30*, 2136−2140.
(35) Hucknall, A.; Rangarajan, S.; Chilkoti, A. *Adv. Mater.* **2009**, *21*, 2441−2446.
(36) Lowe, A. B. *Polym. Chem.* **2010**, *1*, 17−36.
(37) Hoyle, C. E.; Lowe, A. B.; Bowman, C. N. *Chem. Soc. Rev.* **2010**, *39*, 1355−1387.
(38) Themistou, E.; Battaglia, G.; Armes, S. P. *Polym. Chem.* **2014**, *5*, 1405−1417.
(39) Endo, T. General Mechanisms in Ring-Opening Polymerization. In *Handbook of Ring-Opening Polymerization*; Dubois, P., Coulombier, O., Raquez, J-M., Eds; Wiley-VCH Verlag GmbH & Co. KGaA: Weinheim, Germany, 2009; pp 53−63.
(40) Nederberg, F.; Connor, E. F.; Möller, M.; Glauser, T.; Hedrick, J. L. *Angew. Chem., Int. Ed.* **2001**, *40*, 2712−2715.
(41) Moad, G.; Rizzardo, E.; Thang, S. H. *Aust. J. Chem.* **2009**, *62*, 1402−1472.
(42) Moad, G.; Rizzardo, E.; Thang, S. H. *Acc. Chem. Res.* **2008**, *41*, 1133−1142.
(43) Chiefari, J.; Chong, Y. K. B.; Ercole, F.; Krstina, J.; Jeffery, J.; Le, T. P. T.; Mayadunne, R. T. A.; Meijs, G. F.; Moad, C. L.; Moad, G.; Rizzardo, E.; Thang, S. H. *Macromolecules* **1998**, *31*, 5559−5562.
(44) Rosselgong, J.; Armes, S. P. *Macromolecules* **2012**, *45*, 2731−2737.
(45) Rosselgong, J.; Armes, S. P.; Barton, W.; Price, D. *Macromolecules* **2009**, *42*, 5919−5924.
(46) Rosselgong, J.; Armes, S. P.; Barton, W. R. S.; Price, D. *Macromolecules* **2010**, *43*, 2145−2156.
(47) Li, Y.; Armes, S. P. *Macromolecules* **2005**, *38*, 8155−8162.
(48) Rizzi, S. C.; Hubbell, J. A. *Biomacromolecules* **2005**, *6*, 1226−1238.
(49) von Burkersroda, F.; Schedl, L.; Gopferich, A. *Biomaterials* **2002**, *23*, 4221−4231.
(50) Liu, Y.; Wu, N.; Wei, Q.; Cai, Y.; Wei, A. *J. Appl. Polym. Sci.* **2008**, *110*, 3172−3177.
(51) Karlsson, C.; Emanuelsson, K.; Wessberg, F.; Kajic, K.; Axell, M. Z.; Eriksson, P. S.; Lindahl, A.; Hyllner, J.; Strehl, R. *Stem Cell Res.* **2009**, *3*, 39−50.
(52) de Peppo, G. M.; Sladkova, M.; Sjovall, P.; Palmquist, A.; Oudina, K.; Hyllner, J.; Thomsen, P.; Petite, H.; Karlsson, C. *Tissue Eng., Part A* **2013**, *19*, 175−187.
(53) Delaine-Smith, R. M.; MacNeil, S.; Reilly, G. C. *Eur. Cell Mater.* **2012**, *24*, 162−174.
(54) van de Wetering, P.; Zuidam, N. J.; van Steenbergen, M. J.; van der Houwen, O. A. G. J.; Underberg, W. J. M.; Hennink, W. E. *Macromolecules* **1998**, *31*, 8063−8068.
(55) Hutchings, L. R.; Narrainen, A. P.; Eggleston, S. M.; Clarke, N.; Thompson, R. L. *Polymer* **2006**, *47*, 8116−8122.
(56) Luo, C. J.; Stride, E.; Edirisinghe, M. *Macromolecules* **2012**, *45*, 4669−4680.
(57) Tan, S.-H.; Inai, R.; Kotaki, M.; Ramakrishna, S. *Polymer* **2005**, *46*, 6128−6134.
(58) Bhattarai, S. R.; Bhattarai, N.; Yi, H. K.; Hwang, P. H.; Cha, D. I.; Kim, H. Y. *Biomaterials* **2004**, *25*, 2595−2602.
(59) Liang, D.; Hsiao, B. S.; Chu, B. *Adv. Drug Delivery Rev.* **2007**, *59*, 1392−1412.
(60) Nair, L. S.; Laurencin, C. T. *Prog. Polym. Sci.* **2007**, *32*, 762−798.
(61) Rabe, M.; Verdes, D.; Seeger, S. *Adv. Colloid Interface Sci.* **2011**, *162*, 87−106.
(62) Roach, P.; Farrar, D.; Perry, C. C. *J. Am. Chem. Soc.* **2005**, *127*, 8168−8173.
(63) Fischer, D.; Li, Y.; Ahlemeyer, B.; Krieglstein, J.; Kissel, T. *Biomaterials* **2003**, *24*, 1121−1131.
(64) Blanazs, A.; Warren, N. J.; Lewis, A. L.; Armes, S. P.; Ryan, A. J. *Soft Matter* **2011**, *7*, 6399.
(65) LoPresti, C.; Massignani, M.; Fernyhough, C.; Blanazs, A.; Ryan, A. J.; Madsen, J.; Warren, N. J.; Armes, S. P.; Lewis, A. L.; Chirasatitsin, S.; Engler, A. J.; Battaglia, G. *ACS Nano* **2011**, *5*, 1775−1784.
(66) Massignani, M.; LoPresti, C.; Blanazs, A.; Madsen, J.; Armes, S. P.; Lewis, A. L.; Battaglia, G. *Small* **2009**, *5*, 2424−2432.
(67) Christian, D. A.; Tian, A.; Ellenbroek, W. G.; Levental, I.; Rajagopal, K.; Janmey, P. A.; Liu, A. J.; Baumgart, T.; Discher, D. E. *Nat. Mater.* **2009**, *8*, 843−849.
(68) Sawyer, A. A.; Hennessy, K. M.; Bellis, S. L. *Biomaterials* **2005**, *26*, 1467−1475.
(69) Mao, Y.; Schwarzbauer, J. E. *Matrix Biol.* **2005**, *24*, 389−399.
(70) Kilian, K. A.; Mrksich, M. *Angew. Chem., Int. Ed.* **2012**, *51*, 4891−4895.
(71) Kilian, K. A.; Bugarija, B.; Lahn, B. T.; Mrksich, M. *Proc. Natl. Acad. Sci. U.S.A.* **2010**, *107*, 4872−4877.
(72) McMurray, R. J.; Gadegaard, N.; Tsimbouri, P. M.; Burgess, K. V.; McNamara, L. E.; Tare, R.; Murawski, K.; Kingham, E.; Oreffo, R. O. C.; Dalby, M. J. *Nat. Mater.* **2011**, *10*, 637−644.
(73) Huang, J.; Gräter, S. V.; Corbellini, F.; Rinck, S.; Bock, E.; Kemkemer, R.; Kessler, H.; Ding, J.; Spatz, J. P. *Nano Lett.* **2009**, *9*, 1111−1116.